

Microfabrication and experimental characterization of an Out-of-Plane MEMS switch

Angela BARACU¹, Raluca MÜLLER¹, Rodica VOICU¹, Catalin TIBEICA¹,
Adrian DINESCU¹, Marius PUSTAN², and Corina BIRLEANU²

¹National Institute for Research and Development in Microtechnologies – IMT Bucharest, Romania

²Micro & Nano Systems Laboratory, Technical University of Cluj-Napoca, Cluj-Napoca, Romania

E-mail: angela.baracu@imt.ro, Marius.Pustan@omt.utcluj.ro

Abstract. This paper presents an approach to improve the performance of a Micro-Electro-Mechanical (MEMS) switch with vertical movement, manufactured using surface micromachining technology. We focused on the investigations of the critical technological dimensions (gap, thickness of the arms) in order to obtain a released, stable mechanical structure and to avoid the stiction effect of the metallic shapes. Technological experiments, Scanning Electron Microscopy (SEM) investigations, CoventorWare and Comsol simulations were performed in order to investigate the electro-thermo-mechanical behaviour of the switch.

Key-words: MEMS switch, thermal actuator, microfabrication, sacrificial layer.

1. Introduction and preliminary

There are many types of driving mechanisms implemented in microactuators: magnetic, electrostatic or thermal. They are used in different applications for microassembling tools or are incorporated in MEMS like diffraction gratings or gear motors [1]. It is important to obtain small size actuators, compatible with complementary metal-oxide-semiconductor (CMOS) technology, with low actuation voltages.

Magnetic actuators convert the electric current into a mechanical output by employing the Lorentz force equation or the theory of magnetism. They present high actuation force and stroke (displacement), but are manufactured by materials which require more complicated technological steps. Electrostatic actuators operate on the principle of electric charge and the deflection can be accurately controlled.

The electro-thermal actuators are of great interest compared with electrostatic actuators (as comb-drive), due to their high output force, obtained for low input voltages. Between the electro-thermal actuator, based on Joule effect, Chevron type is mostly studied and used [2-4]. A

Chevron actuator is a MEMS device, obtained by micromachining techniques. By applying an actuation voltage to a suspended structure with a pre-bent angle, an in-plane movement will be produced.

In this paper we propose an electro-thermal actuator with vertical movement and parallel suspending beams perpendicular to the central driving structure. The structure has an original design and is fabricated using surface micro-machining processes, similar with those described in [5]. A simple fabrication process, which uses a positive photoresist, S1805, as sacrificial layer ensures a very high reproducibility of the developed structures, compared to conventional MEMS electro-thermal actuators. Moreover, the use of resist as a sacrificial layer reduces the manufacturing costs. The paper is focused on the investigations of the critical technological dimensions (gap, thickness of the arms) in order to obtain a released, stable mechanical structure and to avoid the stiction of metallic shapes. Technological experiments, SEM characterization and electro-thermo-mechanical simulations were performed.

2. Design

The proposed MEMS vertical switch is driven by a metallic electro-thermal actuator. Due to the thermal Joule effect induced in the central mobile part, a movement in the vertical plane will occur and commute the switch from the off stage to on. The thermal driving structure contains a suspended central, rectangular shape connected by 5 pairs of symmetric mobile beams. The gap between the bottom aluminium electrodes and the moving part of the switch is equal with the thickness of the sacrificial layer (in our case photoresist). The geometrical dimensions are as following: central rectangular shape: length $500\ \mu\text{m}$ and width $30\ \mu\text{m}$, lateral beams: length $260\ \mu\text{m}$ and width $5\ \mu\text{m}$, distance between the beams $90\ \mu\text{m}$ and the gap between the two upper and bottom electrodes: $0.5\text{-}1\ \mu\text{m}$ (Figure 1).

When applying a voltage to the actuation electrodes, an electric current passes and due to the electro-thermal effect the driving structure and the beams will heat and deform, moving down and contacting the bottom electrode, signal line (a metal-metal direct current-DC contact). The switch will commute from the off into on stage. When the voltage is removed, the thermal driving structure will go back to the initial position. This motion is produced without any deformation of the central driving beam.

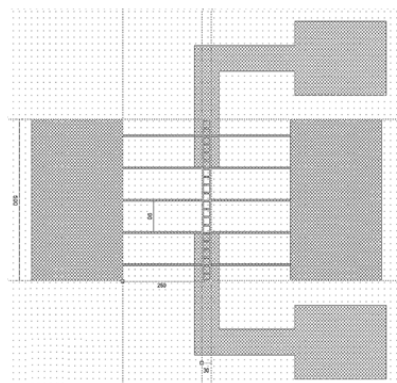


Fig. 1. The MEMS vertical switch configuration.

3. Fabrication

The vertical switch was fabricated using surface micro-machining technology (Figure 2). The manufacturing process involves the use of three photolithography masks: the first is used for the configuration of the aluminium signal line (bottom electrode); the second mask is used to open the windows in sacrificial layer in the actuation electrode areas, while the last mask is used for the aluminium vertical switch structure patterning. The technological flow starts with an n type $525 \mu\text{m}$ thickness, $\langle 111 \rangle$ orientation silicon wafer. A thin film of 300 nm Si_3N_4 , obtained by low-pressure chemical vapor deposition (LPCVD), was used in order to passivate the substrate.

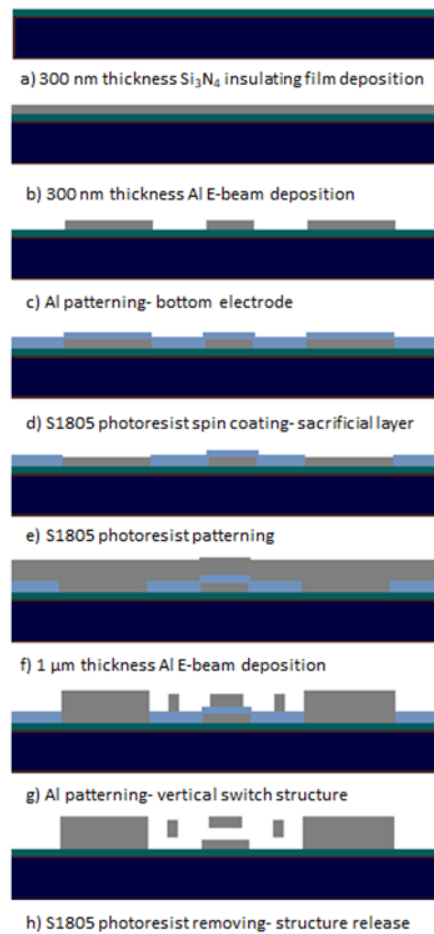


Fig. 2. Fabrication steps of the switch.

The first metal was aluminium, with a thickness of 300 nm, deposited by Electron-beam (E-beam) evaporation. It was patterned using photolithographic process and wet chemical etching. An optical image can be seen in Figure 3 a. We can observe the two rectangular electrodes where will be applied the actuation voltage and the other two electrodes (the signal line) used for the on/off contacts of the switch.

The next processes were the deposition and patterning of a positive photoresist (S1805). Two versions were considered for thickness deposition: 500 nm and 1 μm respectively. This resist is used as a sacrificial layer in order to release the final mechanical MEMS switch structure. By comparison to SiO_2 used as sacrificial layer for conventional MEMS manufacturing, this positive resist has the advantage of easy and low cost fabrication.

After the photoresist was patterned, we removed the unwanted sacrificial layer, in the region of the actuation electrode (Figure 3 b).

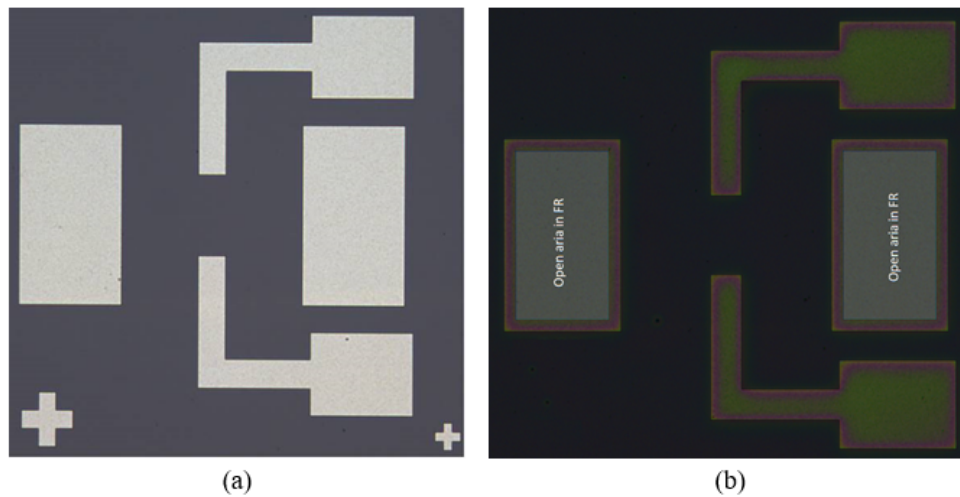


Fig. 3. Optical image of the configured (a) Al bottom electrodes; (b) photoresist sacrificial layer [6].

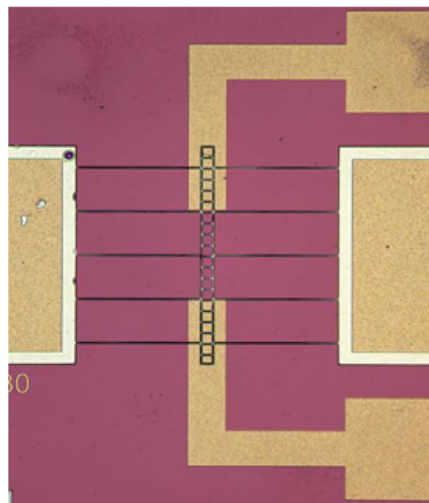


Fig. 4. The top Al configured structure of the vertical switch (before the removal of the sacrificial layer-optical microscope image) [4].

A second aluminium layer of 1 μm thickness was deposited by E-beam evaporation. The vertical switch structure was defined by wet etching of the top metallic layer using the third photolithographic mask. The optical image is presented in Figure 4.

The last step was the removal of the photoresist sacrificial layer and the releasing of the mobile-driven structure of the switch. This process was performed using oxygen plasma etching, which allowed us to avoid the unwanted stiction phenomena, which can occur during classical wet removal between the metals, leading to enhanced reliability of the structures.

4. Simulation

Coupled electro-thermo-mechanical numerical analyses using Finite Element Method (FEM) were performed by CoventorWare and Comsol Multiphysics software packages in order to analyse the behaviour of the structure for an actuation (pull-in) voltage in air. A simplified 3D model (Figure 5) of the structure was considered in simulation. The mesh was defined by parabolic elements. The material properties of aluminium used in simulation are presented in Table 1.

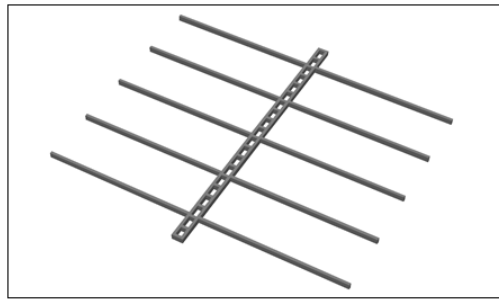


Fig. 5. The simplified 3D model of the structure used in simulation (CoventorWare).

Table 1. The materials properties used in simulations

| Property | Al |
|--|----------------------|
| Young's Modulus (E) [GPa] | 77 |
| Poisson ratio (ν) | 0.3 |
| Coefficient of Thermal Expansion (TCE) [1/K] | $2.31 \cdot 10^{-5}$ |
| Thermal Conductivity for 300 K [pW/($\mu\text{m} \cdot \text{K}$)] | $2.37 \cdot 10^{-8}$ |
| Specific Heat (pJ/kgK) for 300 K | $8.98 \cdot 10^{14}$ |
| Electric Conductivity [pS/ μm] for 300 K | $3.69 \cdot 10^{13}$ |

First, mechanical simulations were performed by applying a pressure of 0.00001 and 0.0001 $\mu\text{N}/\mu\text{m}^2$ respectively, on the top surface of the actuator in order to analyse the out-of-plane displacement of the structure. The obtained maximum values are 0.52 μm and 1.9 μm , respectively (Figure 6).

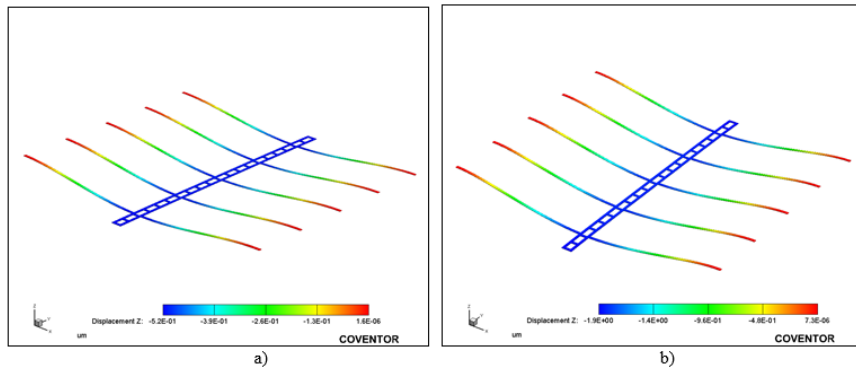


Fig. 6. Vertical displacement of the actuator under pressure: a) $0.00001 \mu\text{N}/\mu\text{m}^2$ applied; b) $0.0001 \mu\text{N}/\mu\text{m}^2$ applied (CoventorWare simulation).

Second, coupled electro-thermo-mechanical analyses were performed for the following boundary conditions: in voltage ($\Delta V=50 \text{ mV}$) between electrodes, convection on external surfaces (air convection coefficient varies between $200 - 1000 \text{ W}/\text{m}^2\text{K}$) and reference temperature ($T=2^\circ\text{C}$). The radiation losses from the device are negligible as compared to the heat loss by convection, since the maximum temperature reached in the actuator is lower than 800°C [7]. The results are presented in Figures 7 – 11 and show that the maximum temperature, around 60°C , occurs in central part of the structure (Figure 7) and the induced out-of-plane displacement reaches $12 \mu\text{m}$ (Figure 8), suggesting that lower applied voltage could be sufficient for the switch to commute from off into on state.

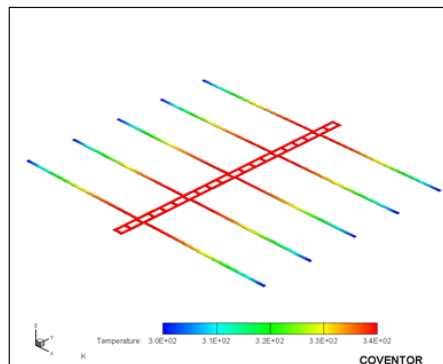


Fig. 7. Temperature distribution in the structure for 50 mV applied (CoventorWare simulation).

In order to find the optimal voltage for actuation, a parametric analysis was performed considering the $1\text{-}200 \text{ V}$ range, considering that, as structural material, aluminium has high melting temperature (655°C [8]) that allows using higher voltage for heating without exceeding the melting point. The variation of electrical current as a function of a voltage is depicted in figure 9 showing that values of less than 80 mA are needed for actuation. Figure 10 presents the variation of maximum temperature 40°C at 25 mV , 60°C at 50 mV and 375°C at 200 mV for lowest convection value. The vertical displacement as a function of voltage (Figure 11) confirms that

for values between 25-30 mV, a displacement higher than $7 \mu\text{m}$ can be achieved. Also, the simulation results show that, at low potential, the convection coefficient does not significantly affect the current, temperatures and vertical displacements reached in the structure (Figures 9-11).

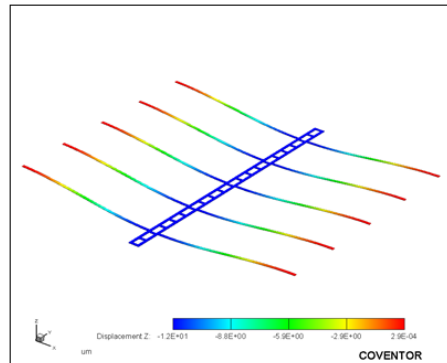


Fig. 8. Out-of-plane displacement for 50 mV applied (CoventorWare simulation).

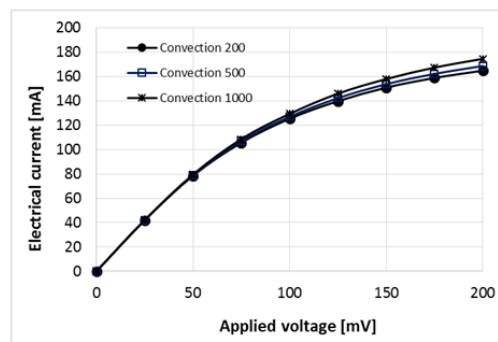


Fig. 9. Electrical current versus the applied voltage (CoventorWare simulation).

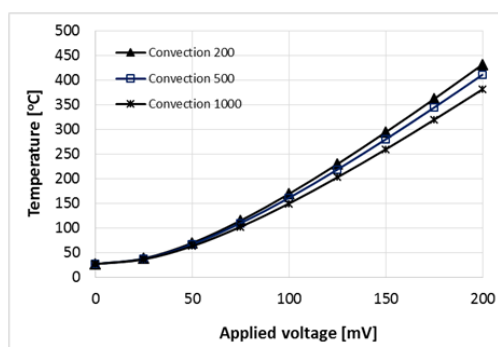


Fig. 10. Variation of maximum temperature reached in the structure as a function of applied voltage (CoventorWare simulation).

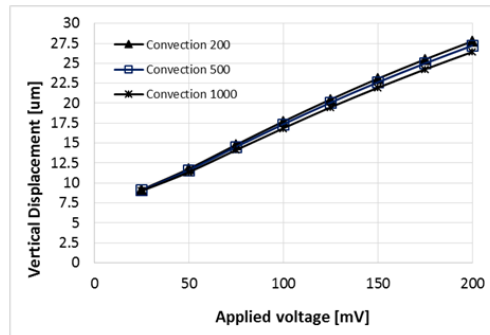


Fig. 11. Out-of-plane displacements for an applied voltage (CoventorWare simulation).

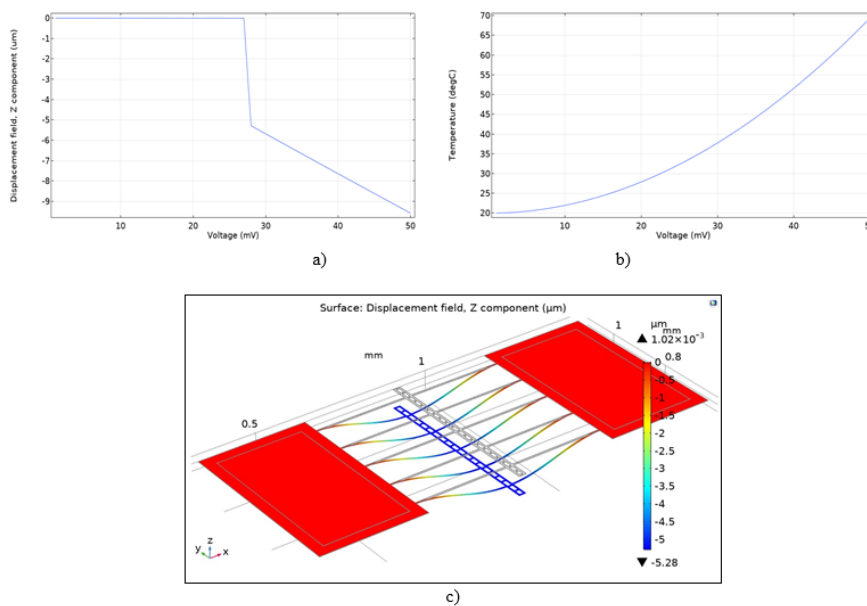


Fig. 12. Simulation results for an applied voltage: a) Out-of-plane displacements; b) Temperatures; c) Detail for the vertical displacement at 28 mV (Comsol simulation).

The variation of vertical displacement (Figure 12a) reveals that it is nearly constant and negligible for potentials up to 28 mV, it has a sharp transition to 5.3 μm between 28-29 mV and linearly increase to 10 μm for 29-50 mV potential range. The variation of maximum temperature as a function of applied potential (Figure 12b) shows that 35°C is reached at 28 mV and 70°C at 50 mV. Both sets of results in terms of displacements and temperature, particularly for 50 mV applied voltage, are similar to the results obtained from CoventorWare and bring additional details on mechanical behaviour at lower voltage. An applied potential of 30 mV is appropriate to ensure the out-of-plane displacement and to commute the switch from off into on state.

The proposed MEMS switch use different materials and a different geometrical configuration (also number, positions of beams) and is hard to compare the simulation results with others in the literature, as in [9] where a chevron microactuator is used to obtain the out-of-plane displacement, being fabricated using SOI.

5. Results and Discussions

In this paper we manufactured two different structures, by changing the depth of the gap (respective photoresist: 500 nm and 1 μm). We studied the fabricated switch using optical and Scanning Electron Microscopy. As can be seen in Figure 13 and 14, in both cases free standing structures were obtained.

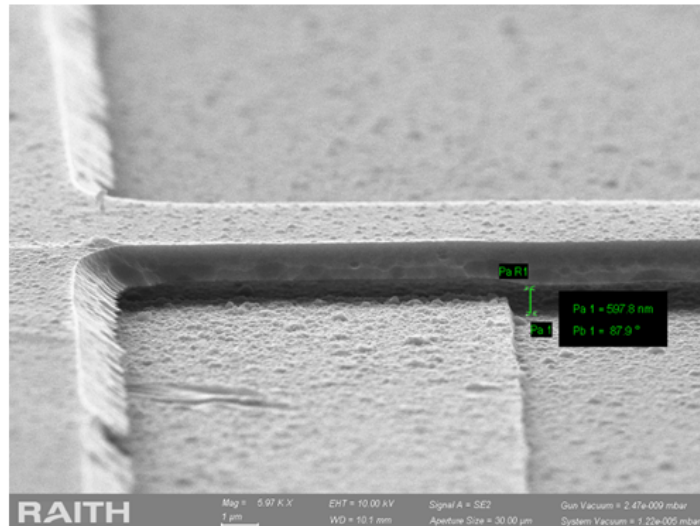


Fig. 13. SEM image of the released beam of the switch for a 500 nm gap.

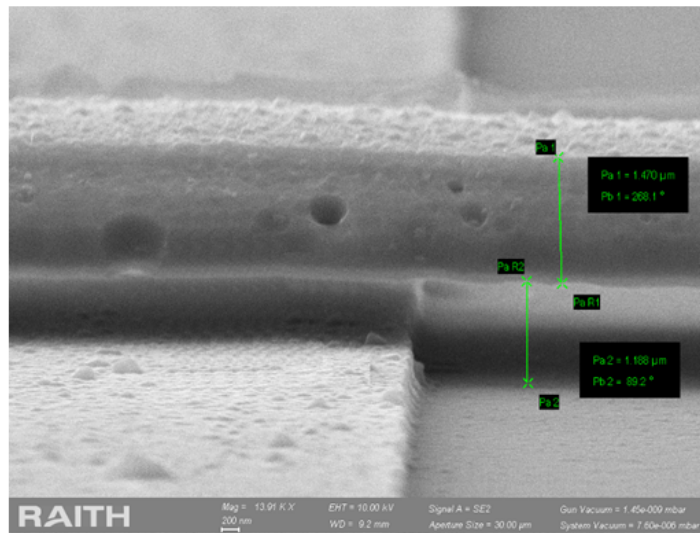


Fig. 14. SEM image of the released beam of the switch for a 1 μm gap [6].

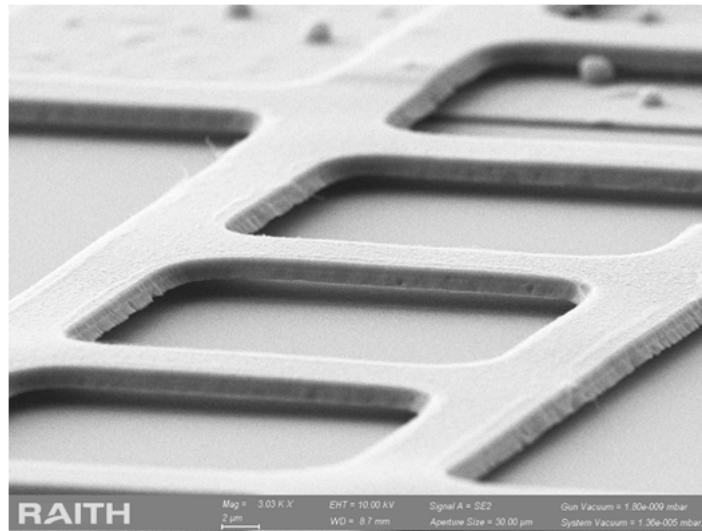


Fig. 15. SEM image of the released central shape with holes and the suspended beam of the switch.

In addition, in the central rectangular shape we designed regular, rectangular holes which enable a fast and complete removal of the S1805 photoresist sacrificial layer, in order to obtain a free, released structure (Figure 15).

6. Conclusions

We presented the manufacturing of a MEMS switch, by surface micromachining techniques, using a photoresist as sacrificial layer. We obtained a released vertical MEMS switch fabricated by a well-controlled process, with two different gap dimensions. The process is relatively simple with good reproducibility. We simulated the electro-thermo-mechanical behaviour of the switch by CoventorWare and Comsol software tools. This structure can be used as electro-thermal-mechanical switch and as test device for investigation of mechanical stiffness and the adhesion force between two metals.

Different stiffness of investigated switch structure can be obtained if the number of the suspended beams is increased, with effect on the acting signal. Moreover, as the stiffness is higher, the restoring force of the mobile electrode from the fixed one increases and the stiction decreases, respectively. The presented switch structure can also be integrated in MEMS applications where a thermal gradient occurs.

Future work will be focused on experimental measurements, which will be compared with different simulation results.

Acknowledgements. This work was supported by a Grant of the Romanian Agency by Scientific Research and innovation CNCS/CCDI UEFISCDI, project PNIII-P2-2.1-PED-2016-1727.

References

- [1] Alex Man Ho KWAN, et al, *Improved design for an Electro-Thermal IN-Plane Microactuator*, Journal of Electromechanical Systems, pp. 586–595, **21**(3), June 2012.
- [2] L. XIUHAN, L. LEIJIE, et.al, *Electro-thermally actuated RF MEMS switch for wireless communication*, Proc. of the IEEE Int. Conf. on Nano/Micro Eng. And Mol. Syst., pp. 497–500, 2010.
- [3] J. SUN, Z LI, et.al, *Design of DC-contact RF MEMS switch with temperature stability*, AIP Advances 5, 041313, pp. 041313-1 - 041313-8, 2015.
- [4] M. PUSTAN, C. BIRLEANU, DUDESCU, R. Muller , A. BARACU, *Integrated thermally actuated MEMS switch with the signal line for the out-of-plane actuation*, Proc. DTIP 2018, pp. 91–94, May 2018.
- [5] A. BARACU, R. VOICU, R. MÜLLER, A. AVRAM, M. PUSTAN, R. CHIOREAN, C. BIRLEANU, C. DUDESCU, *Design and fabrication of a MEMS chevron-type thermal actuator*, AIP Conference Proceedings 1646, **25** (2015), pp. 25–30.
- [6] A. BARACU, R. MÜLLER, R.C. VOICU, M. PUSTAN*, C. BIRLEANU*, A. DINESCU, *Manufacture and investigation of a vertical mems switch*, International Semiconductor Conference (2018), pp. 299–302.
- [7] K. S. COLINJIVADI, J-B. LEE, R. DRAPER, *Viable cell handling with high aspect ratio polymer chopstick gripper mounted on a precision manipulator* Microsyst. Technol. 14 pp. 1627–1633, 2008.
- [8] www.asminternational.org
- [9] Yong-Sik KIM et al, *Creating large out-of-plane displacement electrothermal motion stage by incorporating beams with step features*, J. Micromech. Microeng. **23**(2013) 055008.